MODELLING MATERIAL PROPERTIES LEADING TO THE PREDICTION OF DISTORTION DURING HEAT TREATMENT OF STEELS FOR AUTOMOTIVE APPLICATIONS

Z. Guo, J.P. Schillé – Sente Software Ltd., U.K.
N. Saunders, A.P. Miodownik – Thermotech Ltd., U.K.

ABSTRACT

Heat treatments are widely used in various manufacturing processes to enhance the quality of a product. Distortion induced by heat treatment is a major industrial problem because it critically affects the dimensional accuracy of precision components, which may considerably increase the costs of operations and decrease the quality of core parts. Prediction of distortion induced by heat treatment is difficult because such prediction requires detailed knowledge of the material properties which are normally lacking and difficult to evaluate, especially at high temperatures.

This paper describes the development of a computer model for prediction of the material properties required for distortion prediction. The success of the model is based on accurate description of all the major phase transformations taking place, as well as an accurate calculation of the properties of different phases formed during heat treatment process. The model calculates a wide range of physical, thermophysical and mechanical properties, all as a function of time/temperature/cooling rate or any arbitrary cooling profile. Jominy hardenability prediction was also carried out and shows excellent agreement with experimental data. The model forms part of JMatPro, a new computer software programme for materials property simulation, which allows the present calculations to be carried out via a user friendly interface.

KEYWORDS

Material properties, heat treatment, distortion, residual stress, TTT/CCT diagrams, hardenability

1. INTRODUCTION

Heat treatments are widely used in various manufacturing processes to enhance the quality of a product. However, heat treatment can generate unwanted distortion, a fact that has to be considered when designing the manufacturing process for a given component. Distortion induced by heat treatment is a major industrial problem because it critically affects the dimensional accuracy of precision components, which may considerably increase the cost and time required for product development and decrease the quality of core parts. If distortion can be predicted and controlled then corrections can be made during the machining stage, so that the components reach their final desired shape after heat treatment.

Prediction of distortion induced by heat treatment has generally been based on prior experience or by a trial and error approach. This is because such prediction requires detailed knowledge of the material properties as function of alloy composition and heat treatment procedures, whereas such properties are normally unavailable especially at elevated temperatures.

The stresses within the material can be divided into three types: machining stress, thermal stress and

transformation stresses. Distortion will arise if machining stress is released locally during heating eventually leading to overall distortion. Uneven heating can result in local variations in volume , leading to further stresses and distortion. Transformation stress arises because phases or phase mixtures such as ferrite, pearlite, bainite, martensite and austenite, have different densities. The greatest effect is caused by transformation from austenite to martensite, which causes a marked volume increase. Excessively rapid and uneven quenching can also cause local martensite formation leading to local volume increases which gives rise to stress which may even be high enough to cause quenching cracks.

To predict the distortion caused by the above three types of stress, the following information on materials properties has to be known:

- Phase transformation kinetics, i.e. TTT and CCT diagrams.
- Temperature and microstructure dependent physical and thermophysical properties, such as density, thermal expansion coefficient, and thermal conductivity.
- Temperature and microstructure dependent mechanical properties.

This paper describes some results obtained by the development of new computer software, which can predict the above material properties using as input the alloy composition and heat treatment details only. The success of the model is based on accurate description of all the major phase transformations taking place, as well as an accurate calculation of the properties of different phases formed during heat treatment. Jominy hardenability calculations have also been carried out, using steels for automotive applications as examples. Such output forms part of JMatPro, a newly developed computer software for materials property simulation, which allows the required calculations to be carried out via a user friendly interface.

2. PHASE TRANSFORMATION DIAGRAMS

Knowledge of the TTT and CCT diagrams of steels is important in the processing of steels. Much experimental work has been undertaken to determine such diagrams. However, the combination of wide alloy specification ranges, coupled with sharp sensitivity to composition changes plus a dependency on grain size, means that it is impossible to experimentally produce enough diagrams for generalised use. Significant work has been undertaken over recent decades to develop models that can calculate TTT and CCT diagrams for steels.[1,2,3,4,5)] However, although successful for low alloy steels these models are limited when it comes to more highly alloyed types. One aim of the present work is to develop a model that can provide accurate TTT and CCT diagrams for a much wider range of steels, including medium to high alloy types, tool steels and stainless steels.

This goal has been achieved and JMatPro is now able to calculate TTT and CCT diagrams for steels of all types.[6)] Figure 1 shows the TTT diagrams calculated for four very different types of steels (a) a low alloy 4140 steel, (b) a high carbon, medium alloyed NiCrMo steel, (c) a T1 high speed tool steel and (d) a 13% Cr steel including comparison with experiment for all cases. While Figure 1 provides detailed results for specific alloys, it is instructive to look at the overall accuracy of the calculations. Figure 2 shows a comparison between the experimentally observed times at the nose temperature of the C-curves denoting the start of transformation to ferrite, pearlite and bainite and those calculated from the model. In some cases, particularly for the fast transformation steels, it was not possible to clearly differentiate the nose temperatures for the various transformations. For example, the ferrite, bainite and pearlite transformations appear merged into a continuous C-curve in the experimental work. In such circumstances, the calculated transformation of the fastest phase was taken. The results have been broken down for comparison between British En steels and ASM atlas steels. The dashed lines in Figure 2 represent a deviation of 3 times. The comparison between

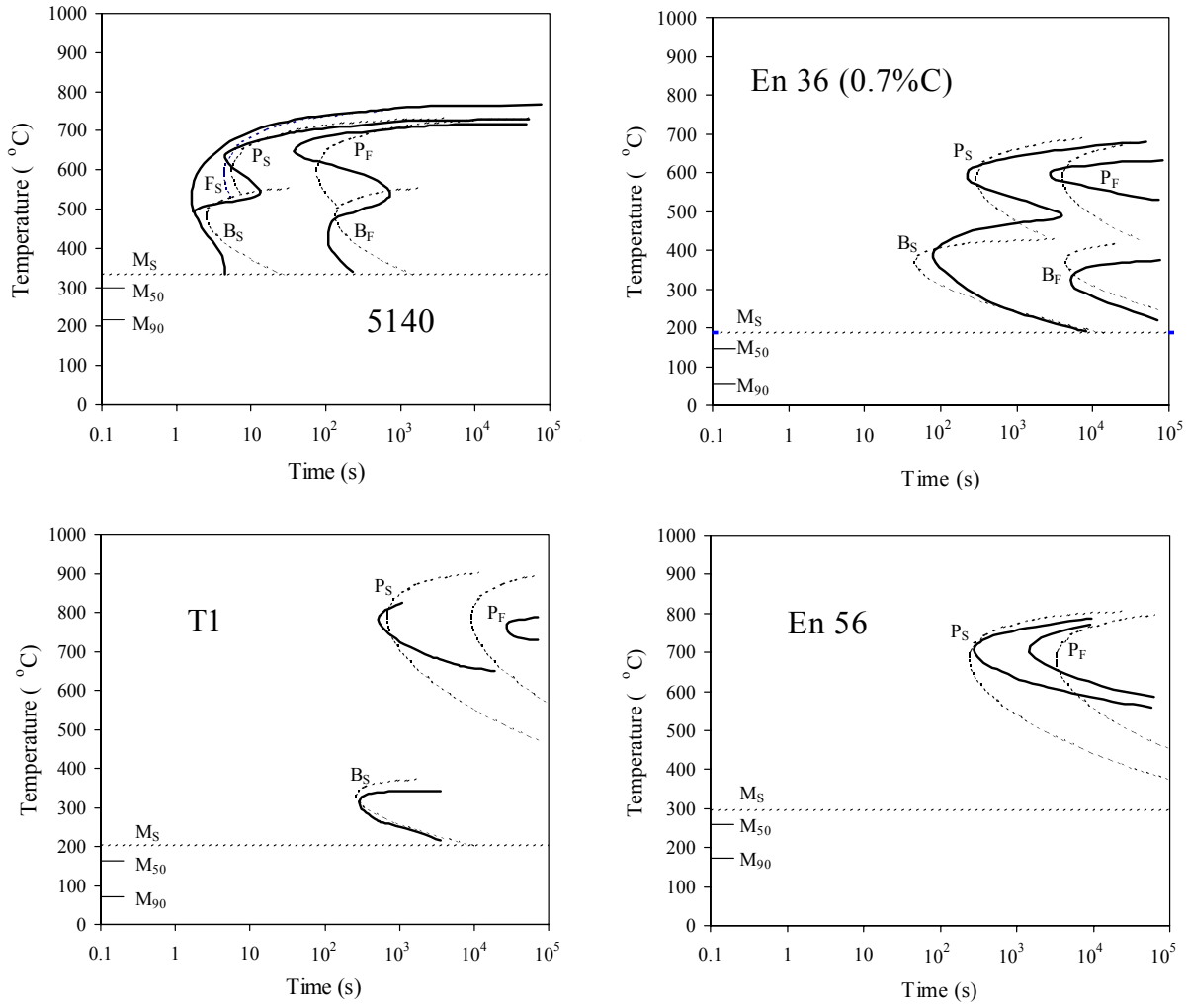

Figure 1. Comparison between experimental (solid lines) and calculated (dotted lines) TTT diagrams for various steels

calculation and experiment is very good and represents a substantial advance over previous models whose range of validity is largely confined to carbon and low alloy steels. Further analysis shows that 80% of calculated results are within a factor of 3 of experiment while almost 90% lie within a factor of 4. To emphasise the high levels of alloying used in the above comparison studies, Table 1 shows the maximum levels of particular elements added as well as the lowest level of Fe in any one alloy.

Table 1. Maximum level of alloying addition in steels used for validation of the model. Also shown is the minimum level of Fe.

	max/min level		max level		max level
Fe	> 75	Ni	< 8.9	W	< 18.6
C	< 2.3	Cr	< 13.3	Al	< 1.3
Si	< 3.8	Mo	< 4.7	Cu	< 1.5
Mn	< 1.9	V	< 2.1	Co	< 5.0

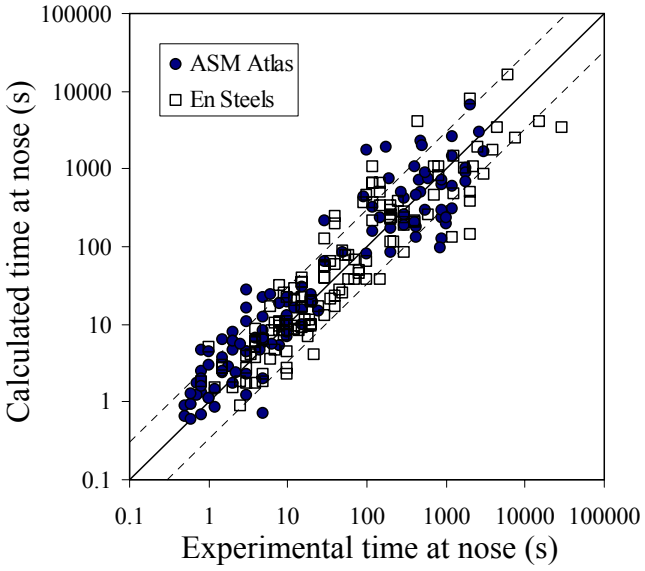

Figure 2. Comparison of calculated and experimental values for the time at the nose of various C-Curves drawn from literature

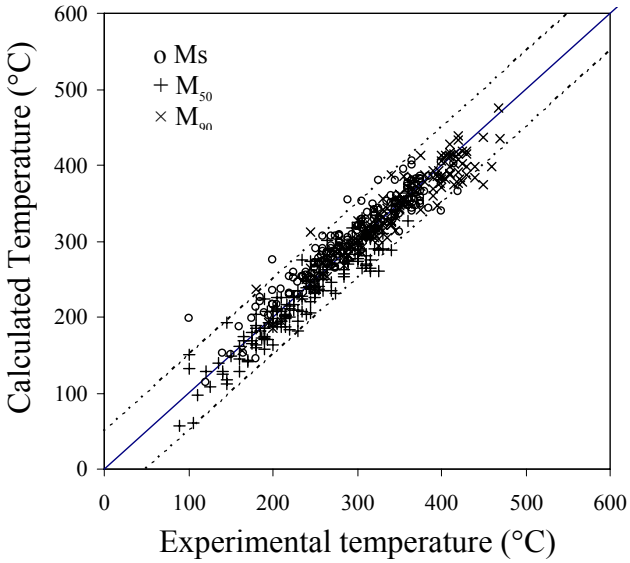

Figure 3. Comparison between experimental and calculated martensite temperatures for various steels.

An accurate description of the martensitic transformation is of great importance because of the large volume change caused by this transformation. The martensite transformation start temperature (Ms) has been modelled, as well as the amount of martensite as a function of cooling below Ms, which in turn enables the temperatures corresponding to 50% (M_{50}) and 90% (M_{90}) of martensite transformation to be determined. Figure 3 shows the comparison between experimental values[7] and calculated Ms, M_{50}, and M_{90} temperatures. As can be seen, the predictions are in very good agreement with experiments.

3. THERMOPHYSICAL AND PHYSICAL PROPERTIES

Thermophysical and physical properties are critical parameters for the prediction of distortions. An extensive database has been created within the development of JMatPro for the calculation of physical and thermophysical properties which is linked to its thermodynamic calculation capability. For each individual phase in a multicomponent system, its properties such as molar volume, thermal conductivity, and Young's modulus are calculated using simple pair-wise mixture models. Once the property of each individual phase is defined, the property of the final alloy can be calculated using mixture models that can account for the effect of microstructure on the final property. Such models, which were developed for two-phase systems, have been extended to allow calculations to be made for multiphase structures. When the properties of the phases are similar, most types of mixture models tend toward the linear rule of mixtures. However, the power of the present models becomes apparent when phases with very different properties exist in an alloy, for instance, in the case of modulus calculations when high levels of carbides or borides are present in relatively soft metallic matrices. Extensive databases of relevant parameters exist for most of the major phases in Al, Fe, Mg, Ni, and Ti alloys. Such databases have been extensively validated against experimental measurements. Utilizing well-established relationships between certain properties (e.g., thermal and electrical conductivity) allows other properties to be calculated without using further databases, so that the following properties can be modelled: volume, density, expansion coefficient, Young's, bulk and shear moduli, Poisson's ratio, thermal conductivity and diffusivity, electrical conductivity, and resistivity.

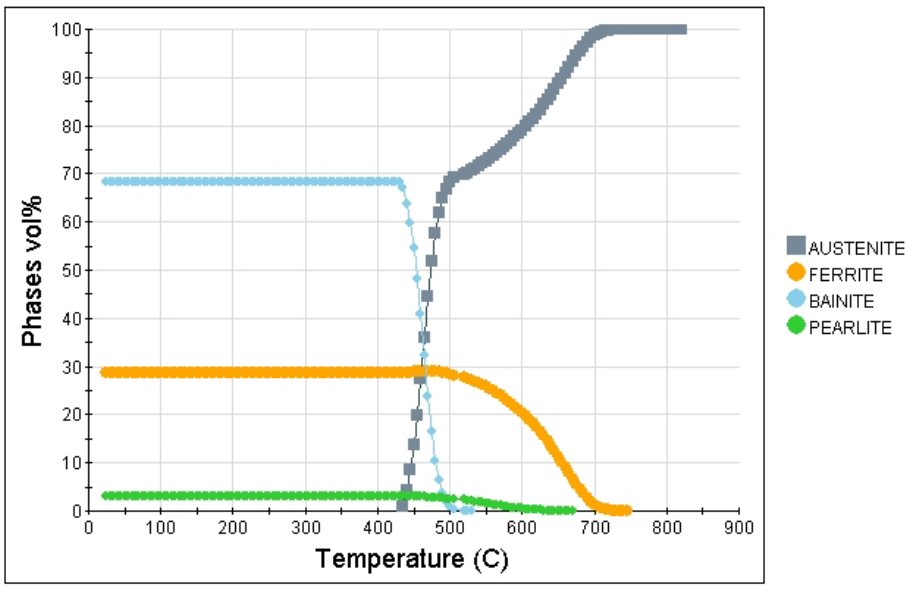

Figure 4. Microstructure evolution in alloy 4140 during cooling at 1 °C/s

The ability of JMatPro to model physical and thermophysical properties has been demonstrated in previous published work for various metallic systems.[8)] Therefore, it is not the intention of this paper to give a full detailed account of how this has been achieved. Interested readers can refer to relevant papers. One should be aware, however, that the properties reported in previous work are either for an alloy after heat treatment (assuming a frozen microstructure below the heat treatment temperature) or during the solidification process, whereas what is going to be demonstrated in this paper is the change of these properties during heat treatment, i.e. to monitor the temperature and microstructure sensitivity of these properties. Once the kinetics of major phase transformations in steels are known, the calculation of material properties during heat treatment is straightforward. First, one calculates the phase evolution during the heat treatment of concern: isothermal holding, continuous cooling, or a any complex cooling path resulting from modern heat treatments. Then by combining the phase constitution with JMatPro's capabilities for calculating the properties of each phase, the overall properties of the alloy during heat treatment can be obtained.

It should be noted that the amount of martensite and bainite are each affected by changes in composition of the parent austenite, which may have resulted from any prior ferrite formation or carbide precipitation at higher temperatures. This has been carefully considered in the present calculation of phase evolution. If there are carbides formed at the start of the transformation, then the composition used is that of the austenite in equilibrium with that carbide, instead of the alloy composition. When ferrite forms, the carbon forced out of ferrite is assumed to be evenly distributed in the remaining austenite phase. Examples given below demonstrate how cooling rate affects the physical and thermophysical properties of steel 4140 with composition Fe-0.98Cr-0.77Mn-0.21Mo-0.04Ni-0.15Si-0.37C (ASTM grain size 7.5). Five cooling rates are set as 100, 10, 1, 0.1, 0.01 °C/s respectively. Figure 4 shows the evolution of various phases during cooling, using 1 °C/s as an example. Martensite does not form in this case. Typical physical and thermophysical properties relevant to the prediction of distortion such as density, linear expansion coefficient, thermal conductivity and enthalpy at different cooling rates are plotted in Figure 5. The properties at 100°C/s and 10°C/s are very close, because the proportion of martensite is over 90% in both cases. Figure 6 shows the comparison between the calculated and experimental quench strain for a 5140 steel, and the error is less than 10%.

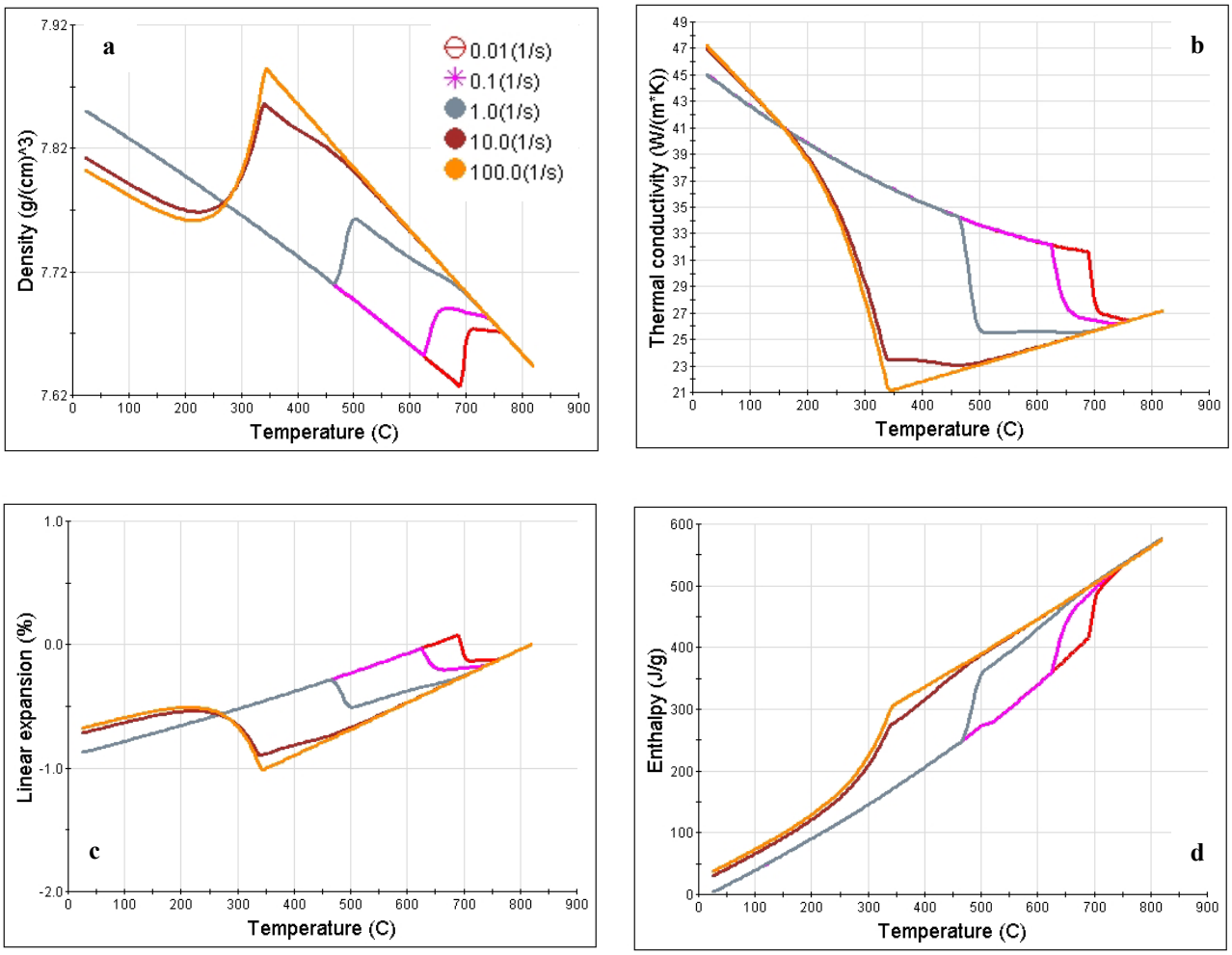

Figure 5. Various properties calculated for a 4140 steel at various cooling rates ranging from 0.01 to 100 °C/s.

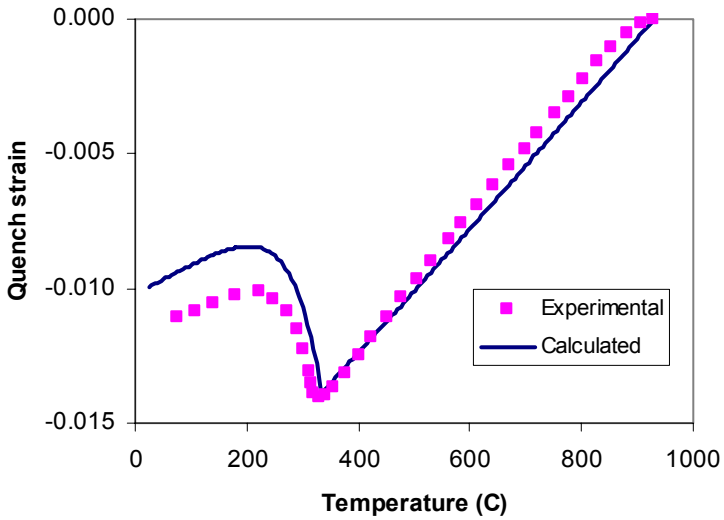

Figure 6. Comparison between the calculated and experimental quench strain for a 5140 steel

4. MECHANICAL PROPERTIES DURING HEAT TREATMENT

The mechanical properties of steels during heat treatment can be calculated following similar procedures to those described in the previous section. Before doing so, the hardness of various phases such as martensite and bainite has to be calculated. Expressions were developed to relate hardness to composition and cooling rate based on the experimental data covering a wide composition range. Figure 7 demonstrates the accuracy of the calculations in comparison with experimental values, using martensite as an example. For austenite and ferrite phases, the strengthening model in JMatPro utilises a generalised pair interaction approach for solid solution strengthening.[9] The classic Hall-Petch equation is employed to account for the dependence of strength on grain size. Using steel 4140 as an example, the influence of cooling rate on yield

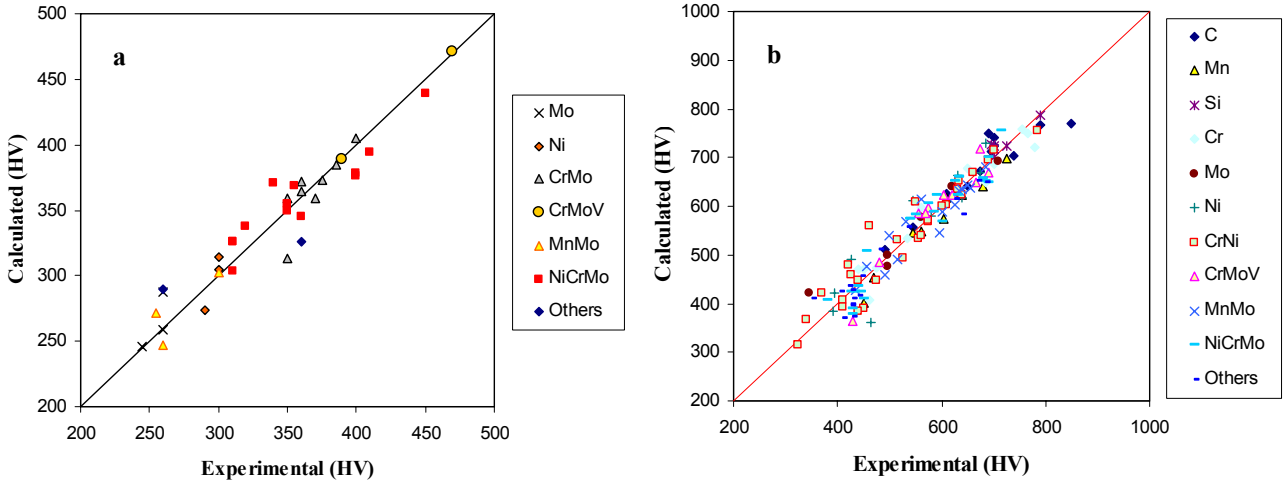

Figure 7. Comparison between experimental and calculated hardness for (a) bainite, and (b) martensite

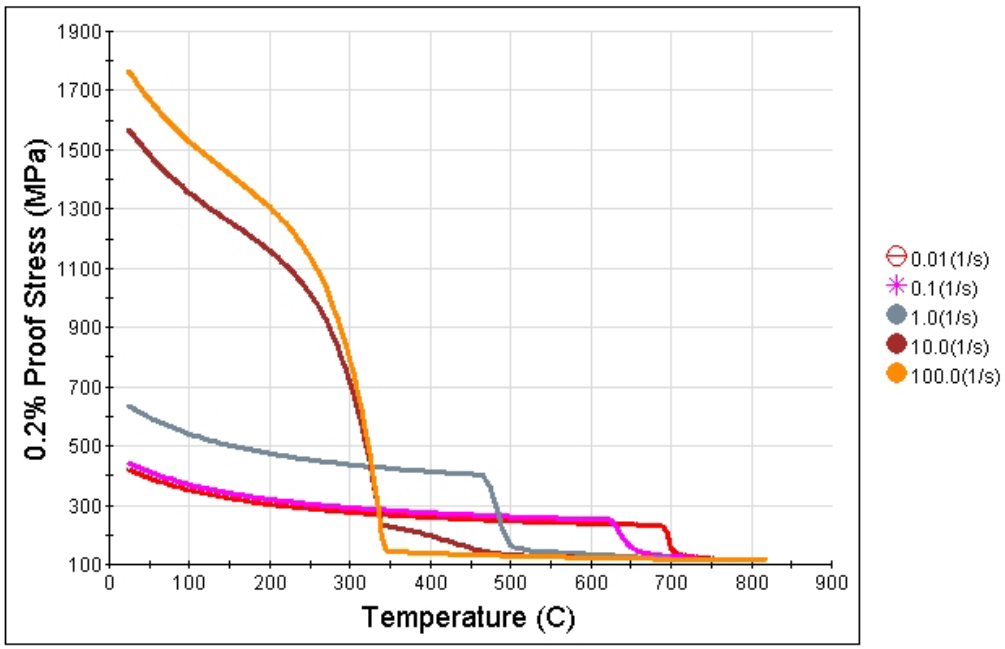

Figure 8. Yield stress for a 4140 steel at various cooling rates ranging from 0.01 to 100 °C/s.

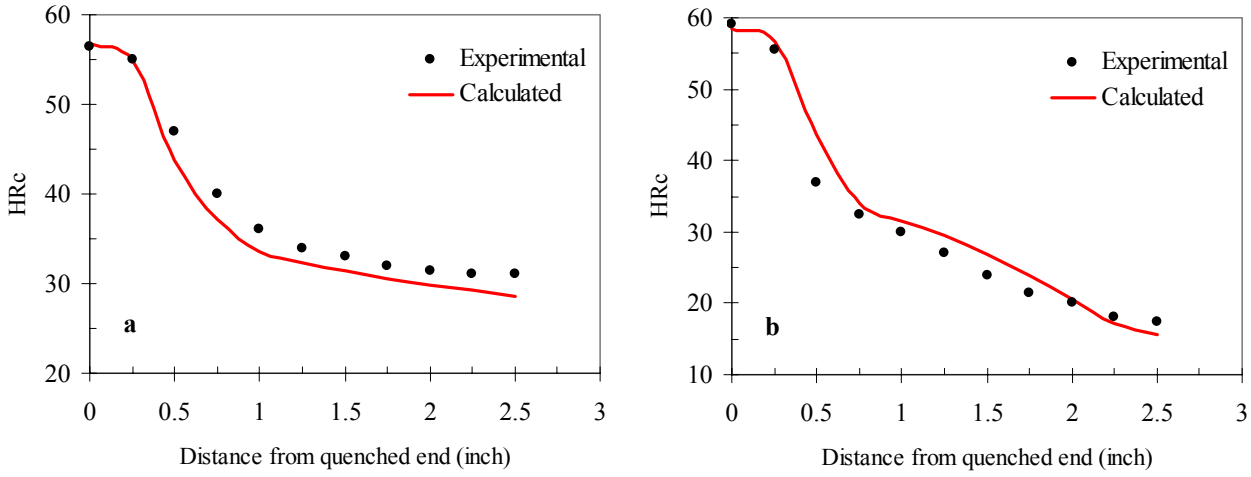

Figure 9. Jominy hardenability comparison between experimental and calculated curve for a) 4140, and b) 5140 alloys

strength and hardness is shown in Figure 8. The strength properties at 100 and 10 °C/s are very close due to the fact that the majority phase is martensite in both cases.

Compared with cooling at a constant rate, Jominy end-quench test results are associated with a more complicated cooling pattern. Accurate prediction of Jominy hardenability curve is therefore of great challenge and importance. The major steps of predicting Jominy hardness using this model are as follows:

1) computing equilibrium phase transformation temperatures and phase composition using a thermodynamic model for the multi-component equilibria in heat treatable steels;
2) calculating the cooling profile for a certain position along the Jominy quenching bar;
3) computing the microstructure evolution at each position along the Jominy bar using transformation kinetics models for austenite decomposition, i.e. the formation of ferrite, pearlite, bainite and martensite; and
4) calculating hardness for a certain position along the Jominy quenching bar.

Again using steel 4140 as an example, the Jominy hardenability curve was calculated and compared with the experimental curve in Figure 9(a).[10] As can be seen that the two curves agree very well. The Jominy hardenability curve of another alloy 5140 (Fe-0.42C-0.93Cr-0.68Mn-0.16Si, ASTM grain size 6.5) was also calculated and agrees well with experimental measurement, Figure 9(b). The curve exhibits two zones: a fast hardness drop from quenching end to 0.75 inch depth, and a slow hardness drop between 0.75 and 2.5 inches. This behaviour can be readily explained by the microstructure change along the Jominy quench bar, Figure 10. It can be seen that the initial fast hardness drop is mainly due to the formation of bainite at the expense of martensite. At depth over 0.75 inch, pearlite starts to form at the expense of bainite (the stronger of the two phases), which leads to the second slow drop in hardness.

6. SUMMARY

Properties relevant to the prediction of distortion induced by heat treatment have been calculated using JMatPro, which embodies new software for materials property simulation and displays the results via a user friendly interface. These properties include TTT and CCT diagrams, physical, thermophysical and mechanical properties, including those at high temperatures, which are

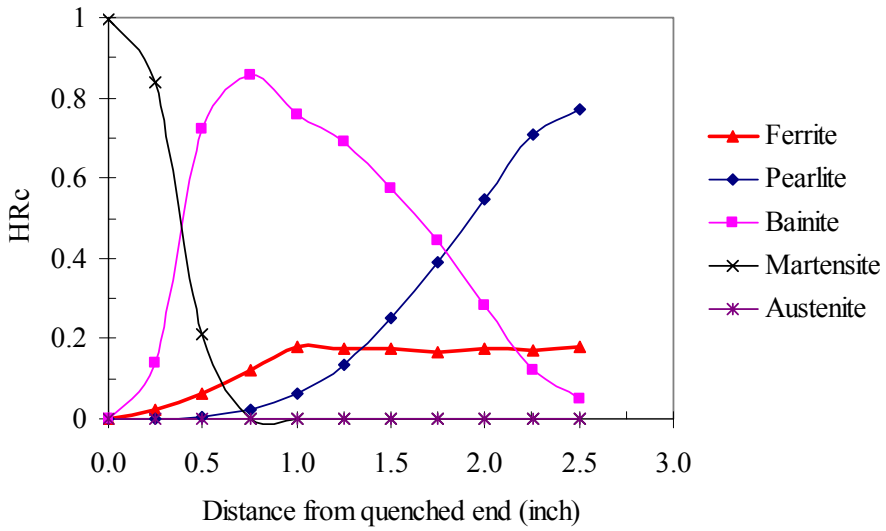

Figure 10. Microstructure change along the Jominy quench bar for a 5140 alloy

normally unavailable. The success of the model is based on accurate description of all the major phase transformations taking place, as well as an accurate calculation of the properties of different phases formed during heat treatment process. The model calculates a wide range of physical, thermophysical and mechanical properties, all as a function of time/temperature/cooling rate or any arbitrary cooling profile. Jominy hardenability prediction for some specific steels used in automotive applications have been used as examples.

REFERENCES

1) J.S. KIRKALDY, B.A. THOMSON, and E.A. BAGANIS, Hardenability Concepts with Applications to Steel, eds. J.S. KIRKALDY and D.V. DOANE, (Warrendale, PA: AIME, 1978), 82.
2) J.S. KIRKALDY and D.VENUGOPOLAN, Phase Transformations in Ferrous Alloys, eds. A.R. MARDER and J.I. GOLDSTEIN, AIME, (Warrendale, PA: AIME, 1984), 125.
3) H.K.D.H. BHADESHIA, Met. Sci. 15, (1981), p.175.
4) H.K.D.H. BHADESHIA, Met. Sci. 16, (1982), p.159.
5) J.L. LEE and H.K.D.H. BHADESHIA, Mater. Sci. Eng. A171, (1993), p.223.
6) N. SAUNDERS, Z. GUO, X. Li, A.P. MIODOWNIK, and J.Ph. SCHILLÉ, The Calculation of TTT and CCT Diagrams for General Steels, Internal report, Sente Software Ltd., U.K., 2004.
7) M. ATKINS, Atlas of Continuous Cooling Transformation Diagrams for Engineering Steels, Sheffield, British Steel Corporation, 1977.
8) http://www.sentesoftware.co.uk/biblio.html
9) X. LI, A. P. MIODOWNIK, N. SAUNDERS, Mater. Sci. Technol. 18, (2002), p.861.
10) AMERICAN SOCIETY FOR METALS, Atlas of Isothermal Transformation and Cooling Transformation Diagrams, Metals Park, Ohio, 1977.